# Beam Scanning Confocal Differential Heterodyne Interferometry

Cheol Song, Tae Joong Kim, Dae-Gab Gweon

Nano opto mechatronics Lab., Dept. of Mechanical Eng, KAIST, Daejeon, 305-701, Korea
(e-mail: feloveyou@kaist.ac.kr, taejoongkim@kaist.ac.kr, dggweon@kaist.ac.kr)

*Abstract* - This paper presents a new approach to the design of confocal differential heterodyne interferometer (CDHI) which is a combination of differential heterodyne interferometer (DHI) with confocal laser scanning microscopy (CLSM). The CDHI can measure a step height over a quarter of wavelength of the light source, which can not be accurately measured by DHI and CLSM respectively. The approach is that it utilizes a beam scanning method instead of transporting a sample to be measured. The measurement results carried out for samples having step height are found to be comparable in precision with those of the measured by commercial scanning electron microscopes.

Key words - Confocal laser scanning microscopy, Differential heterodyne interferometer, Beam scanning, Compensation of OPD

## I. INTRODUCTION

Nowadays, because of advancement of nano-technology and bio-technology; demands on technology about surface manufacturing, precision measurement and positioning have been increased. Accordingly, lots of precision measurement systems have been developed, and some of them used optical metrology methods in the field of opto-mechatronics. These systems have some merits such as high resolution and a nondestructive effect to specimen. A special application is confocal laser scanning microscopy (CLSM) characterized by high resolution images due to confocal aperture i.e. pinhole, optical sectioning to serially produce thin sections of a specimen, and 3D reconstructions of a variety of biological specimens. Also differential heterodyne interferometer (DHI) which is constructed according to the common-path scheme goes well with the accurate measurement of the step height

and also have the high-resolution performance obtained by its stability against environment noises [1, 2]. However, the DHI can measure phase only from 0 to $2\pi$ radians because of sinusoidal nature of optical interference. Therefore, the measurable step height of the DHI is limited to one quarter of the wavelength of the light source. In order to solve this problem, wavelength-scanning scheme applied to differential heterodyne interferometer was developed a few years ago [3]. Another technique, the DHI combined with CLSM has also been building [4]. The step height over one quarter of the wavelength of the light source can be measured by the confocal differential heterodyne interferometer (CDHI), where the CLSM performs the coarse measurement and the DHI performs fine measurement [5]. But most of its researches were focused on stage scanning method or sample scanning scheme. It takes a lot of time to measure and often creates vibration and noise due to movement of the stage. In this paper, we propose a confocal differential heterodyne interferometry (CDHI) with the beam scanning method that can measure a step height over one quarter of the wavelength of the light source. However, the beam scanning CDHI has difficulty in measuring the step height of the sample directly, because needless information originates from different optical paths of two optical probe beams traveled through optical system components during beam scanning. This unnecessary information was compensated by a precision flat mirror. The proposed beam scanning CDHI was found to obtain similar measurement result compared to measurement result (199 nm) of a commercial scanning electron microscope in the middle of the field of view.

## II. DESCRIPTION OF THE PROPOSED SYSTEM

### A. Differential Heterodyne Interferometer (DHI)

For many years, optical interferometer has been studied by many workers to measure delicate differences in surface profile. It is possible to measure the topography in sub-nanometer level by using optical interferometric techniques [6]. Among these, differential heterodyne interferometer (DHI) has a good point for non-contact characterization of micro-objects and surface profiling [7]. Also DHI is able to measure a step height and line width of a sample with high resolution. Its principle is founded on illumination of the sample with two focused laser beams separated by a distance comparable to the size of the beam spots. DHI measures optical phase difference between the two beams, which is obtained by changing the distance between the two focal spots on the

sample. The distance is not only dependent on the focal spot size but also on the sample shape. Thus it is well known that the differential heterodyne method is useful for measuring small changes in phase including information of the surface profile. Its high sensitivity results from the phase measurement of the beat signal produced by two parallel incident beams whose frequencies are slightly different from each other [8]. In addition, DHI based on common path scheme having same optical path of two beams[9], has a strong point compared to non-differential interferometers as it is less sensitive to environmental disturbances, especially high vibration [10].

The schematic diagram of differential heterodyne interferometer is shown in Fig.1. Laser emits a coherent beam with two frequency components $f_1$ and $f_2$ respectively, which are linearly polarized with two polarization states orthogonal to each other. The beam is decomposed into two beams, A and B traveling through the beam separation plate (BSP). The beam A with frequency $f_1$ is reflected in PBS and mirror $M_1$ . The beam A with frequency $f_1$ turned back to the PBS, however, is able to pass through a polarizing beam splitter (PBS), because the beam passed through the quarter wave plate two times. The other beam A with frequency $f_2$ is reflected by the sample and the PBS. And then two frequency components of the beam A superposing themselves, are detected by $D_A$ as AC signal $I_A$ . The beam B at a distance d apart is also detected by $D_B$ as AC signal $I_B$ :

$$I_A \approx \cos(2\pi f_d t + \phi_A),\ I_B \approx \cos(2\pi f_d t + \phi_B) \qquad (1)$$

where $f_d$ is the difference between frequency $f_1$ and $f_2$ . $\phi_A$ and $\phi_B$ are also defined as $4\pi n L_A / \lambda$ and $4\pi n L_B / \lambda$ , respectively. Here $L_A$ is the path difference of the beam A in two interferometric arms and $L_B$ is the path difference of the beam B in two interferometric arms. $\lambda$ is the wavelength of the optical source, n is the refractive index of the air. If there is a height difference h between A and B in a sample, the measurable step height of the sample is defined below from $\phi = \phi_B - \phi_A = 4\pi n h / \lambda$ :

$$h = (\lambda / 2n)(\phi / 2\pi) = (\lambda / 2n)(m + e) \qquad (2)$$

Here m and e are integer numbers and the remainders of interference fringes, respectively. The height h is detected as same value e, even though it is a multiple of $\lambda/2n$ [11]. The measurable step height in differential heterodyne interferometer is reduced as $\lambda/4n$ because of $2\pi$ ambiguity added by sign confusion of optical path difference.

### B. Confocal Scanning Laser Microscopy (CSLM)

While the first idea of confocal scanning microscopy was proposed by Minsky in 1957, a decade later Eggar and Petran designed and produced a purely analogue mechanical confocal scanning microscopy. In the late nineteen seventies, the single beam confocal laser scanning microscopy was developed in many laboratories with the advancement in computer technology, laser and digital signal and image processing. And it was used to measure bio-medical and material samples. Especially, the major turning point for many biologists was the publication of six papers in 1985 that proved the power of confocal laser scanning microscopy. Two years later, Oxford-shire Company produced the first commercial confocal laser scanning fluorescence microscopy [12].

The principle of the confocal laser scanning epi-fluorescence microscopy is illustrated in Fig.2. Laser beam from the light source pinhole aperture is reflected by the dichromatic mirror and is focused by an objective lens to a diffraction limited spot at the focal plane within the 3D specimen. Only emissions from the in–focus plane can be detected by the photomultiplier after passing through the dichromatic mirror and the detector pinhole aperture. Other emissions from out of focus planes are stopped by the detector pinhole aperture; it is not contributed to the measurement image any more.

Confocal laser scanning microscopy is divided into two categories; a beam scanning type and a stage scanning type according to scanning mechanism. The beam scanning type can scan a sample rapidly and is resistible to vibrations and disturbances from environment. But it has a complex system configuration and distorted images compared to stage scanning type.

Confocal laser scanning microscopy has better resolution than conventional optical microscopy and improved signal to noise ratio by rejecting unwanted information using a pinhole aperture. The major characteristic of confocal laser scanning microscopy is to obtain 3D information of a sample. Such information can be achieved by using “optical sectioning” to cut a slice having thickness of 0.5um even though the sample thickness is over 50um. It can be achieved by controlling the position of the step motor along the sectioning direction. However, confocal

laser scanning microscopy has a limited spectral range of fluorescence emission because illumination by a high power laser is harmful to the bio-sample, and its commercial products are very expensive.

An ideal point object is formed as amplitude point spread function on the image plane of confocal laser scanning microscopy. Instead of it, however, intensity point spread function can determine the resolution of the system, which is visible to the naked eye. This value can be measured whenever a point object is defocused along the optical axis. It is often called "Axial response"; the depth of field of a confocal microscopy is determined by FWHM (Full width at the half-maximum height) of axial response. The FWHM of a confocal microscopy is reduced relative to that of conventional optical microscopy by a small but significant factor of about 1.4 [13].

In conventional optical microscopy, the size of the diffraction-limited focal spot is defined as the radius of the Airy disk $r_{Airy}$ , which is the distance between the central maximum and the first minimum (zero crossing) in the Airy disk:

$$r_{Airy} = 0.61\frac{\lambda}{NA_{obj}} \tag{3}$$

Here $\lambda$ means the emitted light wavelength, $NA_{obj}$ is numerical aperture of the objective. Therefore, the lateral resolution is defined by the well-known Rayleigh criterion, according to which two diffraction-limited focal spots are said to be just resolved when the distance between two focal spots becomes larger than $r_{Airy}$ [14].

In the case of confocal fluorescence microscopy, lateral (or axial) extent of the point spread function is reduced about 30%; the width of the Airy disk along the axial and lateral direction compared to wide field optical microscopy becomes narrower:

$$r_{Airy} = 0.4\frac{\lambda}{NA_{obj}} \tag{4}$$

as shown in the above equation, lateral resolution is improved by using a high numerical-aperture objective and a short-wavelength laser light source. Axial resolution can also be explained likewise. There are various equations to express axial resolution according to microscopy configurations. The equation below is commonly used to describe axial resolution for the confocal microscope configuration:

$$r_{axial} = 1.4 \frac{\lambda \eta}{NA_{obj}^{\ 2}} \qquad (5)$$

where $r_{axial}$ represents a moving distance of the object lens to locate the focal spot at the first minimum intensity point viewed along the direction of 3D diffraction space. It is proportional to the wavelength $\lambda$ and index of refraction $\eta$, and is inverse-square of numerical aperture of the microscope objective lens [15].

### C. Proposed Confocal Differential Heterodyne Interferometry (CDHI)

In this paper, to measure specimen dimensions quickly, we suggest beam scanning confocal differential heterodyne interferometer (CDHI). The schematic diagram and photograph of the CDHI are depicted in Fig.3 and Fig.4, respectively. The 633nm He-Ne laser beam (Model 1125, JDS Uniphase), after passing through the beam expander, heads toward the acousto–optical deflector (AOD) (AA.DTS.X, AA OPTO-ELECTRONIC). Notice that the direction of light polarization traveling through the linear polarizer is parallel to the plane of incidence (it is said to be p-polarized) in order to maximize the output efficiency of the acousto-optical deflector. The parallel beam which enters the Bragg cell or AOD leaves with the change of polarization state at an angle of 90 degree. According to the driving voltage, Bragg cell driver outputs the RF signal with frequency $f_{RF}$. If the AOD is operated only by the RF signal, only one beam leaves out. However, if an amplitude-modulated signal is applied to the AOD, two linearly polarized first-order beams with slightly different frequencies leave out, due to the diffraction effect and Doppler effect of the Bragg cell. The Doppler effect is caused by the signal modulation with two frequencies $f_{RF} \pm f_{\mathrm{mod}}$, as shown in Fig.5. Here, the frequency $f_{RF}$ controls x-axis scanning of the optical beam probes whereas the frequency $f_{\mathrm{mod}}$ controls the distance between the two focal spots on the sample. Referring to Fig.3, the half-wave plate can change the polarization direction of the two beams traveling through the AOD so that only about 20 percent of light intensity can be reflected at the polarizing beam splitter (PBS) after the beams go through relay optics. Two first-order beams are divided into two polarized beam components in PBS, respectively. The s-polarized beam components reflected in PBS, after passing through the iris, are detected by PD 1 as a reference beat interference signal. After the p-polarized beams are reflected by the two galvano mirrors, they illuminate a specimen through an objective lens, and become two minute spots on different positions of the

sample. The p-polarized beams reflected from the sample become s-polarized, because the beams pass through the quarter-wave plate two times, therefore the beams turned back to the PBS are reflected. After the beams are reflected in the beam splitter (BS) again and passed through the iris, are detected by PD 3 as a sinusoidal signal called a probe beat interference signal, which is measured as different values according to various sample shapes, in contrast with the invariant reference beat interference signal detected in PD 1. Lock-in amplifier is able to acquire sample information by measuring such a phase difference between the reference signal and probe signal. The other beams transmitted in BS, after passing through the collecting lens and the small size pinhole, are detected by PD 2 as a confocal intensity signal. The positions of the pinhole and focal point in the sample have confocal relation.

The proposed system uses the principle of DHI. Therefore, the reference beat interference signal in PD 1 is detected as intensity $I_1$ with unchanged phase. And the probe beat interference signal in PD 3 is detected as intensity $I_3$ including sample information [16]

$$\begin{aligned} I_1 &\propto \cos[(\omega_1 - \omega_2)t + \psi_{ref}] \\ I_3 &\propto \cos[(\omega_1 - \omega_2)t + \psi_{probe} + \delta\phi] \end{aligned} \tag{6}$$

where $\psi_{ref}$ and $\psi_{probe}$ are electrical phases related to respective channels, $\delta\phi$ means the phase difference between the two beams including sample information. Thus optical phase difference between the two beams on the sample gives sample information. The distance between the two focal beams and their focal size are critical parameters of measurement performance. To measure a step height precisely, the distance between two focal beams should be larger than the radius of the focal spot. In case of measuring the line width of the sample, the distance between two focal beams should be smaller than line width [17].

## III. MEASUREMENT PRINCIPLE AND COMPENSATION

### A. Step Height Measurement

Phase measuring interferometers have better axial resolution than confocal scanning laser microscopy, but the limitation of its measurable height is reduced to λ/4 due to 2π ambiguity of the sample with the step height. When the step height is measured by only interference signal, the optical phase difference is the same value whenever the step height is a multiple of 2π as shown in equation (7). Therefore, the true height $\theta$ can not be determined due to unknown integer m:

$$\theta = 2m\pi + \phi \qquad (7)$$

where $\theta$ means the true height of a sample, m is an integer, and $\phi$ ($-\pi < \phi < \pi$) is the optical phase difference.

In this paper, the 2π ambiguity is overcome by measuring and analyzing both confocal and interference signals simultaneously. The procedure is shown as two steps in Fig.6 [18]. At first, as the precision stage moves along the z-axis, the axial response of confocal intensity signal is measured by PD 2. When the focal plane is located at the top of the sample (z=0), the maximum confocal intensity signal is detected by PD 2. The more is the distance from zero (z=0), the less is the confocal intensity. The sample location along the z–axis is a function of the confocal intensity. In the next step, galvano mirrors scan the sample positions (x, y). The confocal intensity signal and interference signal are measured by PD2 and PD3 simultaneously and respectively. If the reflectivity of the sample is same over the whole surface of the sample, the step height of the sample position (x, y) can be obtained by comparing the confocal signal with the axial response in the first step. However, it is coarse height information due to noise, etc. Therefore, fine height information can be achieved by comparing the reference beat interference signal with the probe beat interference signal using a lock in amplifier. Finally, the value of integer m can be determined by the confocal signal. Exact height information $\theta$ can be decided by the interference signal $\phi$.

### B. Compensation Procedure

The proposed CDHI is able to deflect two first-order beams by using two galvano mirrors. Both the confocal intensity signal and interference signal are obtained simultaneously. The acquirement of interference signal is accomplished by optical heterodyne method. These beams have different optical paths in the optical system

components during beam scanning. The beam scanning CDHI yields unnecessary optical path difference between two beams before they arrive on the sample. The interference signal of the two beams can not have a precision value of the step height. Therefore, the compensation of optical path difference ('OPD 1') caused by the optical system components is needed. The OPD 1 is measured by setting a highly accurate flat mirror on the bottom surface of the specimen. Both roughness and flatness of the mirror is crucial for the compensation. In the next step, another optical path difference ('OPD 2') is measured by replacing the flat mirror with the specimen. However, the interference signal of the OPD 2 is a combination of both OPD1 caused by the optical system components and optical path difference of the step height of the specimen. Therefore, the compensated result is achieved by subtracting OPD 1 from OPD 2.

## IV. MODELING AND ANALYSIS

### A. Finite Ray Tracing (FRT)

Here, a method to trace the optical path numerically is presented. Although a finite ray tracing spends more time to calculate than Gaussian ray tracing, it can be performed easily by a computer. Finite ray tracing is a basic numerical calculation with Gaussian ray tracing and calculation of the Seidel aberrations in the design of optical systems.

As shown in Fig.7, a ray travels from the point P of the coordinates system $I_A$ to the point S on the spherical surface of the coordinates system $I_B$. The distance between the point P and S is C, the distance in straight line along the optical axis is d. Origin of the coordinates system $I_A$ is located at point A ; origin of the coordinates system $I_B$ is located at point B. Let the coordinates of P be ( $x_{-1}$, $y_{-1}$, $z_{-1}$ ), and of S be (x, y ,z). When the point P is viewed in coordinates system $I_B$ , its coordinates ( $\underline{x}$ , $\underline{y}$ , $\underline{z}$ ) are related to x, y, z respectively:

$$\begin{aligned} x &= \underline{x} + LC \\ y &= \underline{y} + MC \\ z &= \underline{z} + NC \end{aligned} \qquad (8)$$

Where L, M and N are unit vectors in the direction of vector C. Here $\underline{x} = x_{-1}$, $\underline{y} = y_{-1}$ and $\underline{z} = z_{-1}$ -d (origin of the new coordinates is shifted as d.) F and G are defined as below; C is also decided as below:

$$F = \frac{(\underline{x}^2 + \underline{y}^2 + \underline{z}^2)}{r} - 2\underline{z}$$
$$G = N - \frac{L\underline{x} + M\underline{y} + N\underline{z}}{R} \qquad (9)$$
$$C = \frac{F}{G + \sqrt{G^2 - F/R}}$$

And the next propagation vector $(L', M', N')$ is determined by Snell's law which is applied to the spherical surface of the coordinates system $I_B$ . Therefore, if both the vectors and points on the surface of the optical system can be calculated continually, all-optical paths can be traced**.**

### B. Analysis of OPD 1 Using Finite Ray Tracing

Before the step height of a sample is accurately measured by the two beams, the optical path difference between the two first order beams, OPD 1, is occurred by the optical system components, lens, scanner, etc. The OPD 1 can be simulated by the finite ray tracing. In fact, this is the theoretical value to be compensated in the sample measurement.

The configuration of the proposed optical system is simplified as shown in Fig.8, in order to be applied to the finite ray tracing. The measurement range is limited to 100 um x 100 um. A perfect flat mirror instead of a real sample is applied to the calculation to obtain the OPD1 caused only by the optical system components. The OPD 1 is simulated by considering that two first-order beams travel from x-axis galvano mirrors to the flat mirror including the opposite direction. It is assumed that the distance between two focal spots in the middle of field of view is about 1um. The simulated characteristics of OPD 1 are shown in Fig.9. As the scanning range (field of view) increases, the OPD 1 becomes larger nonlinearly and rapidly. In order to avoid $2\pi$ ambiguity occurred before the measurement of the sample, the scanning range should be restricted. When the x-axis galvano mirror works only, the OPD 1 is shown in Fig.10. When the y-axis galvano mirror works only, the OPD 1 is also shown in Fig.11. If the slopes are compared in the two figures, the magnitude of OPD 1 occurred only by the x-axis

galvano mirror is bigger than that by the y-axis galvano mirror. The reason is that the initial positions of the two first-order beams are the same as the x-axis scan direction. And the OPD 1 is zero if both galvano mirrors does not work at all. The OPD 1 obtained experimentally is shown in Fig. 12. The experimental result of maximum OPD 1 is about 30~36 nm, which is different from that of the theoretical simulation result even though the tendency is similar. This is due to optical system components which are not considered in simulation and the arrangement error of optical system components in experiment.

## V. EXPERIMENT AND MEASUREMENT RESULTS

### A. Experimental Process

When proposed CDHI measures the step height, the distance between the two focal spots on the sample is critical parameter. Two first order beams traveling through the Bragg cell are located at the focal plane after passing through both the relay optics and objective lens. Therefore, the distance between the two focal spots is dependent on magnification of the relay optics and focal length of the objective lens. Thus the distance between the two focal spots on the sample was determined by considering magnification of the relay optics and focal length of the objective as it is shown in Fig.13. The distance between the two focal spots is proportional to the modulation frequency driven into the Bragg cell. The modulation frequency and the angle between the two beams are related by sine function. But there is a linear relationship between them, because the angle between the two beams is very small when they are focused on the sample through the objective lens. In addition, in order to measure the step height of the sample precisely, the distance between the two focal spots on the sample should be larger than the radius of the focal spot. Therefore, the modulation frequency of 0.32 MHz is used to the measurement of the step height.

In order to compensate the OPD 1, the scan position on the flat mirror must be the same that the position on the sample. Therefore, the feedback signal of the galvano mirror scan position, confocal signal, and interference signal were synchronized on C++ program. Data acquisition board (PCI-6036E, National Instruments) was used to obtain the feedback signal of the galvano mirror position, to output the analogue input control signal of the galvano mirror, and to acquire the confocal signal. The axial response on the sample was measured by using a

picomotor (New focus) which can move the sample precisely along the optical axis. The interference signals were obtained by a dual phase lock-in amplifier (LIA 150, Becker & Hickl GMBH).

The measured sample configuration is illustrated in Fig.14. The measurement was accomplished by scanning in the middle of the field of view using the x-axis galvano mirror. The exact distance of beam scanning was decided by calculating rotation angle of the galvano mirror, magnification of the relay optics and focal length of the objective lens. In addition, the true scan distance was calibrated by comparing with measurement results of a sample which has a known dimension.

Non-differential optical interferometers have the $2\pi$ ambiguity when the step height of the sample is over a half of the wavelength of the optical source. But differential interferometers have the $2\pi$ ambiguity when the step height of the sample is over a quarter of the wavelength of the optical source with the ambiguity of falling edge and rising edge in the sample. Therefore, the step height of the period $\lambda / 4$ can be analyzed by the confocal intensity information.

### B. Measurement Result

Axial response at the middle of the field of view is as shown in fig.15. The numerical apertures of the objective and collecting lens are 0.45 and 0.25 respectively. And the diameter of the pinhole is 25 um. This axial response can be used sufficiently because it has 7 um bandwidth of axial direction corresponding to the intensity between 0.3 and 0.9 of the right side of the curve which has a high sensitivity. However, when the confocal intensity signal is measured, the sample is located at the focal plane of the objective. The confocal intensity signal is placed on the curve's line which has a bad sensitivity at the axial response. Therefore, the position of the pinhole was defocused into the photodiode such that the measured confocal signal was located on the high sensitivity line of the axial response as shown in Fig.15. As shown in Fig.16, the left-shifted curve was the axial response which has a high sensitivity at the focal plane (z=0). And the axial response was fitted by a polynomial equation of $20^{th}$ order because the data composing curve line was not continuous. Thus the height information corresponding to the measured confocal signal was calculated on the left-shifted axial response. So to speak, the coarse step height of the sample was decided by comparing the confocal intensity signal with the axial response as shown in Fig.17. The asymmetry of confocal intensity in falling edge and rising edge was caused by both tilt of the sample to the

optical axis and small dissymmetry of the sample shape. The measured step height was 237 nm, between a quarter and a half of the wavelength of the optical source, even though the interference signal has the $2\pi$ ambiguity.

The OPD 1 caused by system components has nothing to do with the confocal intensity signal as it is only related to the compensation of interference signal. The final measurement was achieved by the compensation procedure using a high 3-axis precision stage in order to place the sample on the flat mirror position. The compensation result of measurement in the middle of the field of view is shown in Fig.18

The true step height of the sample can not be decided by the interference signal due to the $2\pi$ ambiguity, but it can be decided by analyzing the confocal intensity signal in addition to the interference signal. The step height at the middle of the field of view can be decided by both confocal and interference signal as illustrated in Fig.19. Maximum phase difference of the inference signal in the falling edge is 135.67 degrees. The step height by confocal signal is 237 nm and the interference signal is located between $\lambda/4$ and $\lambda/2$. The falling edge corresponding to 135.67 degrees is 197.2 nm and the rising edge to 198.7 nm is 133.99 degrees likewise. The measurement at the middle of the field of view produces similar value, 199 nm measured from a commercial scanning electron microscope. Furthermore, from the experiment, it was found that the beam scanning CDHI took just a few minutes to measure the specimen height.

## VI. CONCLUSION

This paper proposes the beam scanning confocal differential heterodyne inteferometry. It is composed of a differential heterodyne interferometer and a confocal laser scanning microscopy. Throughout this work, the beam scanning CDHI can be suggested as a useful system in terms of measuring the step height over a quarter of wavelength of the light source. Because the different optical paths of two beams cause the interference signal to have the needless information OPD 1, its compensation has been accomplished. The experiment result shows a similar value as compared to the measurement result of a commercial scanning electron microscope in the middle of the field of view. Thanks to the beam scanning, the measurement speed is even better than the stage scanning method.

## VII. REFERENCE

[1] H.J.Tiziani, A.Rothe, and N.Maier. 1996. Dual- wavelength heterodyne differential interferometer for high-precision measurements of reflective aspherical surfaces and step heights. Applied optics. 35: 3525-3533.

[2] H.J.Tiziani, N.Maier, and A. Rothe. 1996. Scanning differential heterodyne interferometer with acousto-optic deflectors. Optical communications 123: 34-40.

[3] Sheng-Hua Lu, Ching-I Chiueh, and Cheng -Chung Lee. 2002. Differential wavelength-scanning heterodyne interferometer for measuring large step height. Applied optics. 41:5866-5871.

[4] Dejiao Lin, Zhongyao Liu, Rui Zhang, Juqun Yan, Chunyong Yin, and Yi Xu. 2004. Step-height measurement by means of a dual-frequency interferometric confocal microscope. Applied optics. 43:1472-1479.

[5] Tae Joong Kim, Seung Woo Lee, Dae Gab Gweon, Suk Won Lee, Kwang Soo Kim. 2004. Precision measurement of large step height using confocal differential heterodyne interfeormetry (CDHI). Euspen 4th international conference. 282-283.

[6] Michael G.Somekh, M.Salim Valera, and Roland K.Appel. 1995. Scanning heterodyne confocal differential phase and intensity microscope. Applied optics. 34: 4857- 4868.

[7] IM Akhmedzhanov, D V Baranov and E M Zolotov. 2003. Object characterization with a differential heterodyne microscope. Journal of optics A: pure and applied optics. 5: S200-S206.

[8] Shinichi Komatsu, Hiroyuki Shara, and Hitoshi Ohzu. 1990. Laser scanning microscope with a differential heterodyne optical probe. Applied optics. 29:4244-4249.

[9] See C W, Appel R K, Somekh M G. 1988. Scanning differential optical profilometer for simultaneous measurement of amplitude and phase variation. Applied physics letters. 53:10-12.

[10] Michael G.Somekh, M.Salim Valera, and Roland K.Appel. 1995. Scanning heterodyne confocal differential phase and intensity microscope. Applied optics. 34:4857- 4868.

[11] Sheng-Hua Lu, Ching-I Chiueh, and Cheng -Chung Lee. 2002. Differential wavelength -scanning heterodyne interferometer for measuring large step height. Applied optics. 41:5866-5871.

[12] C.J.R. Sheppard and D.M. Shotton, 1997. Confocal Laser Scanning Microscopy, BIOS Scientific Publishers.

[13] C.J.R. Sheppard and D.M. Shotton, 1997. Confocal Laser Scanning Microscopy, BIOS Scientific Publishers.

[14] Eugene Hecht, 2002. Optics (fourth edition), Addison Wesley.

[15] http://olympusconfocal.com/theory/resolutionintro.html . 2004

[16] Haeyang Chung, L.M. Walpita, and William S.C. Chang. 1986. Simplified differential phase optical microscope. Applied optics. 25:3014-3018.

[17] Taejoong Kim, Seungwoo Lee, and Dae-Gab Gweon. 2005. High precision measurement of 3D profile using confocal differential heterodyne interferometer. Journal of the optical society of korea. 9: 22-25

[18] Taejoong Kim, Seungwoo Lee, and Dae-Gab Gweon. 2005. High precision measurement of 3D profile using confocal differential heterodyne interferometer. Journal of the optical society of korea. 9:22-25

# List of the figures

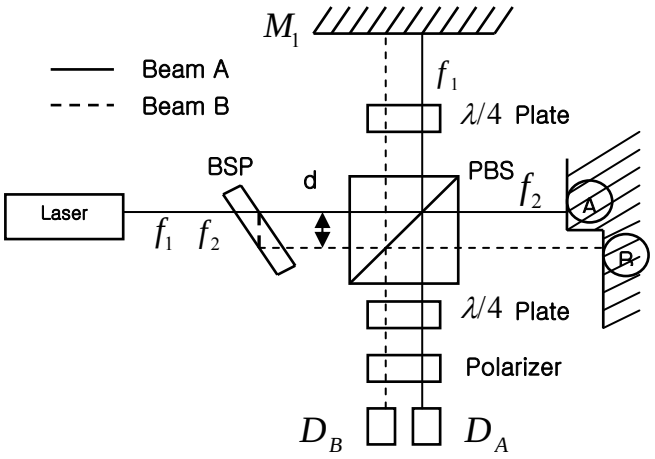


Figure.1 Schematic diagram of the differential heterodyne interferometer.

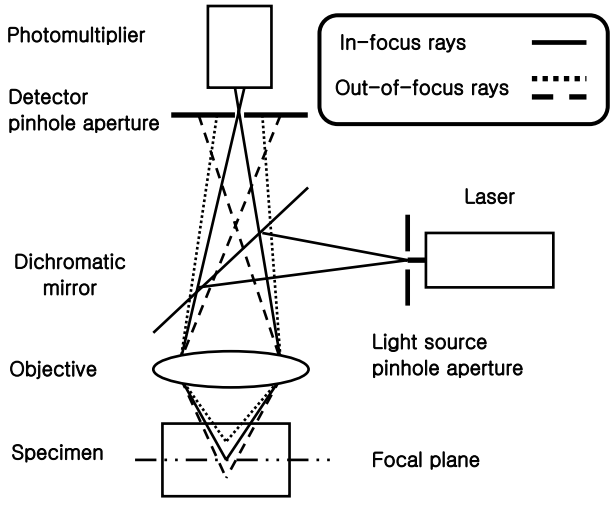


Figure.2 Schematic diagram of the confocal laser scanning epi-fluorescence microscopy.

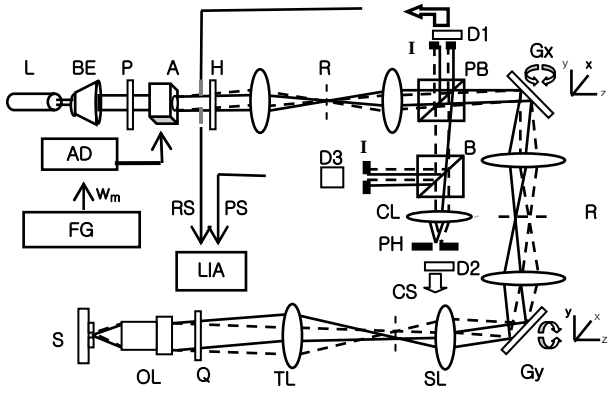


Figure.3 Schematic diagram of the beam scanning confocal differential heterodyne interferometer (CDHI): laser(L), beam expander(BE), polarizer(P), acousto-optical deflector(A), acousto-optical deflector driver(AD), function generator(FG), half wave plate(H), relay optics(R), iris(I), PD1(D1), polarizing beam splitter(PB), x-axis galvanometer(Gx), y-axis galvanometer(Gy), scan lens(SL), tube lens(TL), quarter wave plate(Q), objective lens(OL), sample(S), beam splitter(B), collecting lens(CL), pinhole(PH), PD2(D2), confocal intensity signal(CS), PD3(D3), reference beat interference signal(RS), probe beat interference signal(PS), lock-in amplifier(LIA).

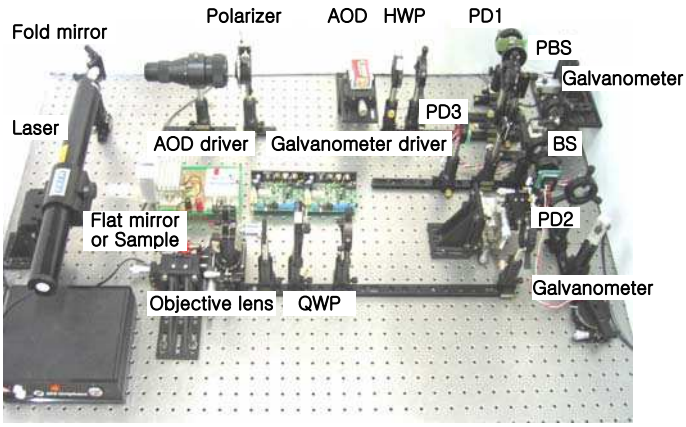


Figure.4 View of the beam scanning CDHI.

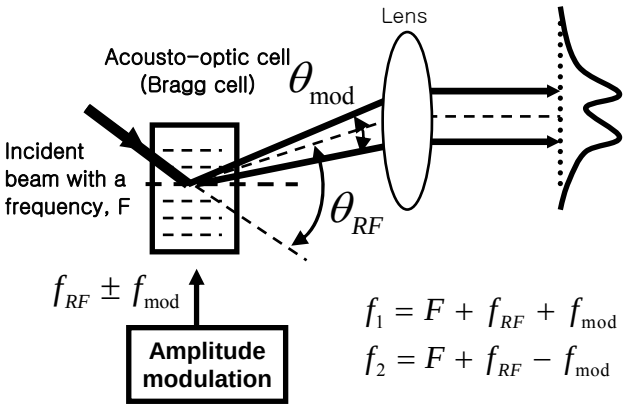


Figure.5 Generation of two first-order beams

from the acousto optic cell (Bragg cell)

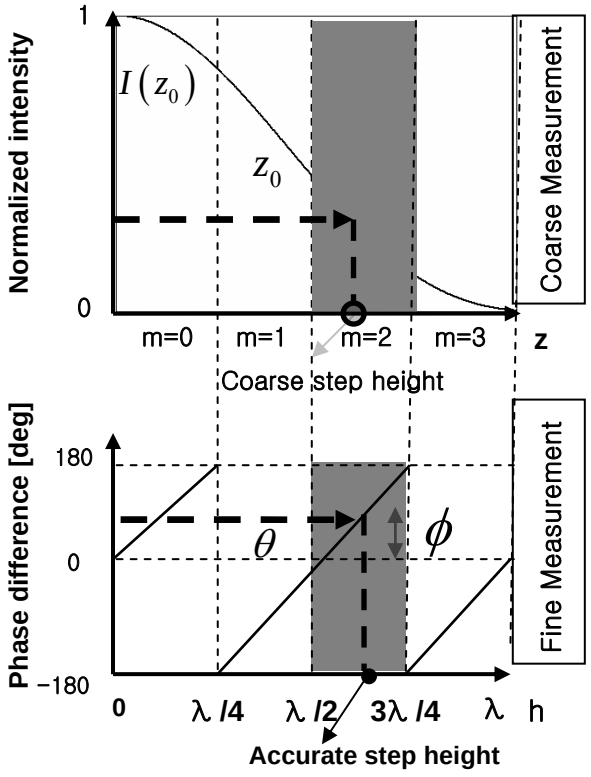


Figure.6 Procedure to measure the

specimen over λ/4 step height.

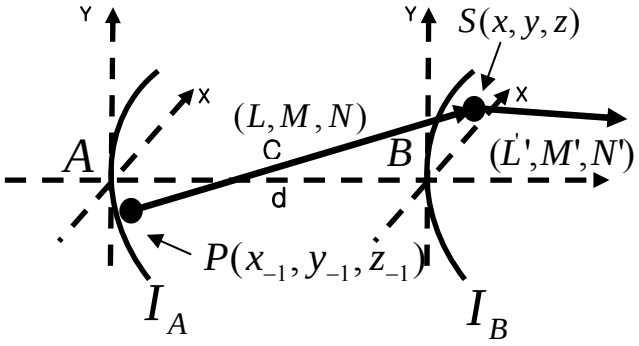


Figure.7 Finite ray tracing.

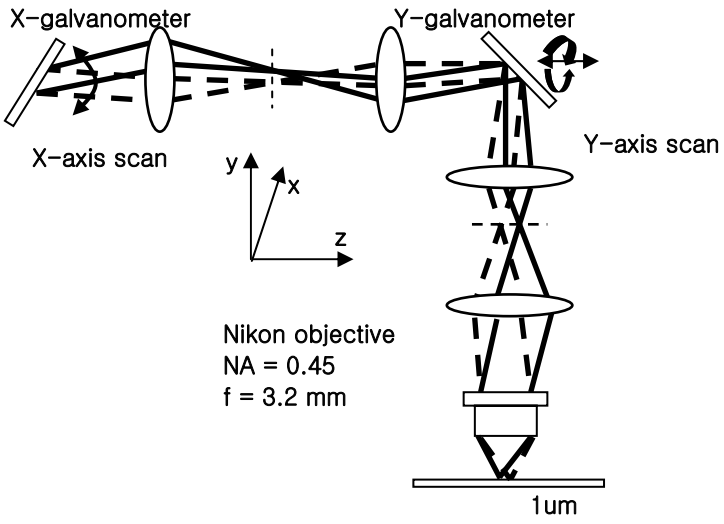


Figure.8 Simulation condition of the finite ray tracing.

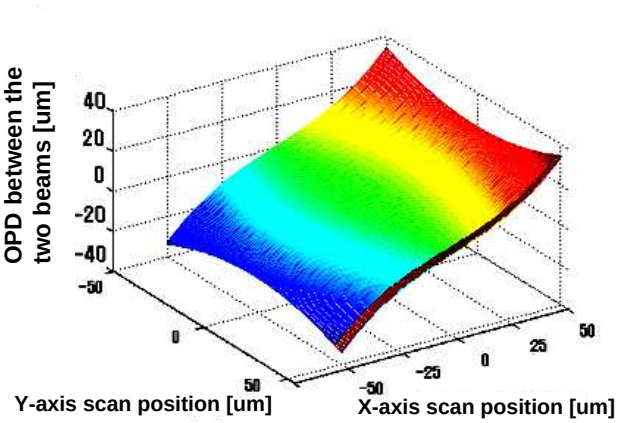


Figure.9 Optical path difference (OPD 1) between the two first-order beams simulated by the finite ray tracing.

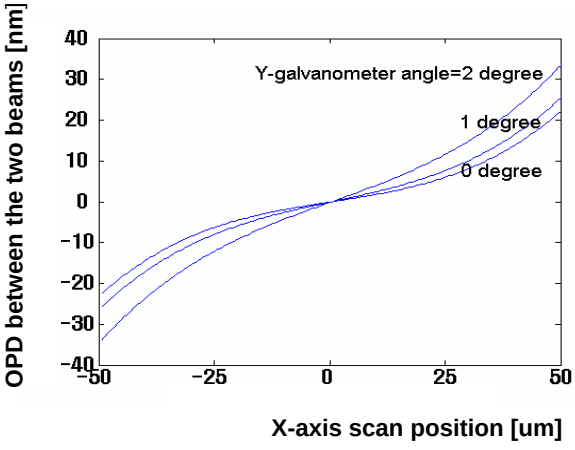


Figure.10 Optical path difference (OPD 1) viewed from the x-axis.

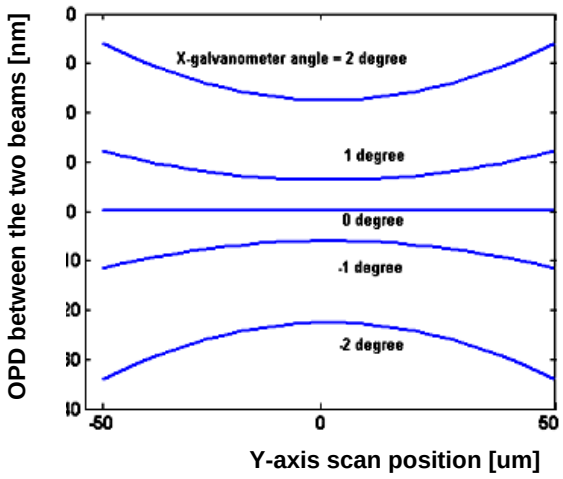


Figure.11 Optical path difference (OPD 1) viewed from the y-axis.

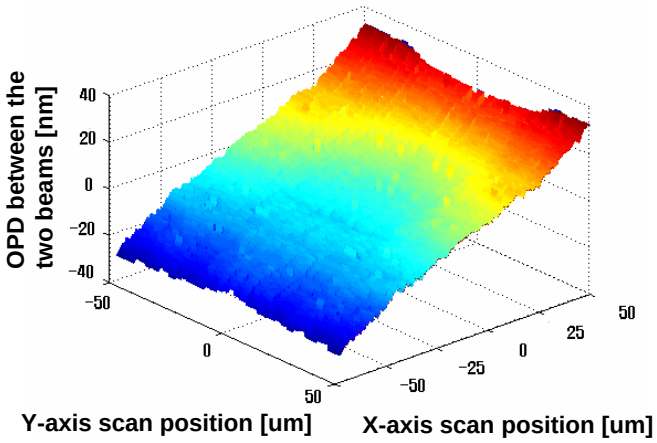


Figure.12 Optical path difference (OPD 1) obtained experimentally.

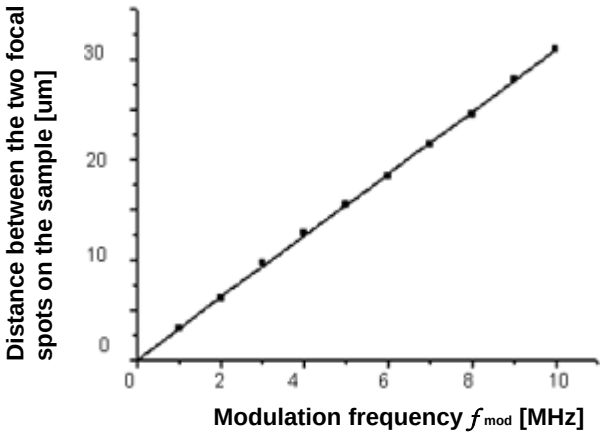


Figure.13 The distance between the two focal spots on the sample vs. modulation frequency

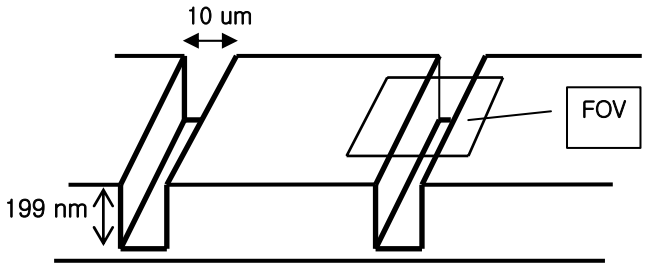


Figure.14 Simple illustration of a sample to be measured

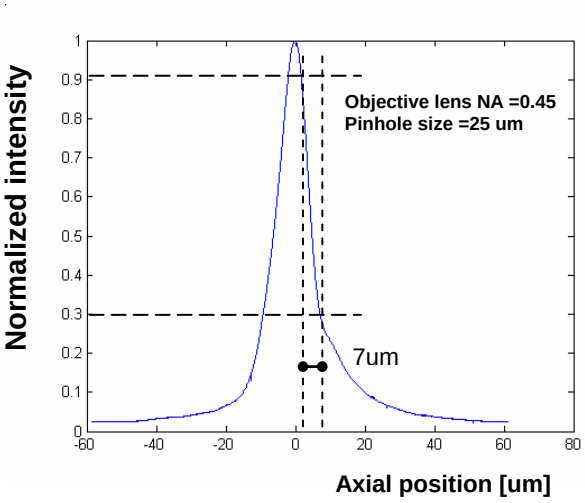


Figure.15 Axial response in the middle of the field of view

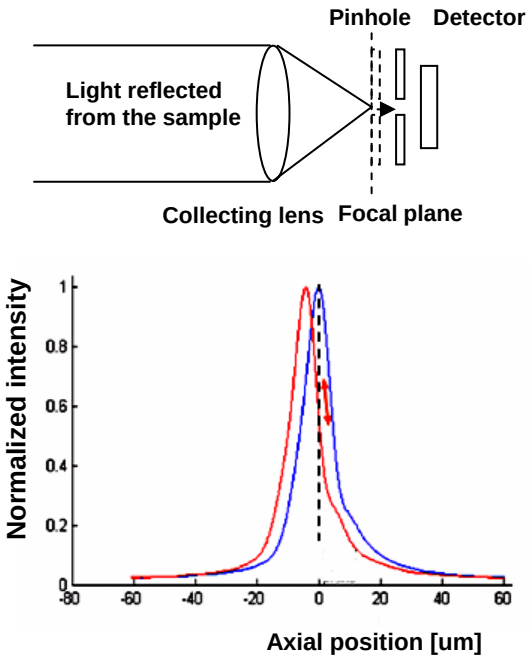


Figure.16 Axial response by defocusing

a pinhole into the detector

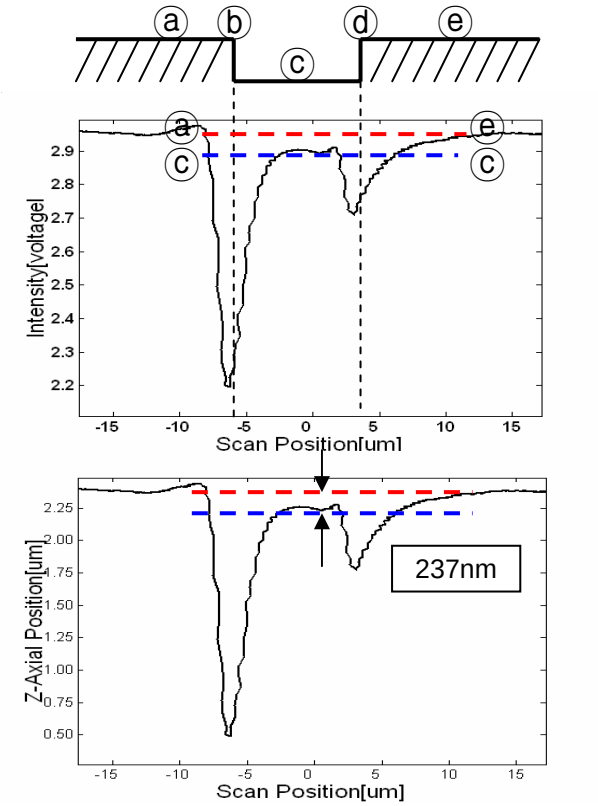


Figure.17 Confocal intensity signal analysis in the middle of the field of view.

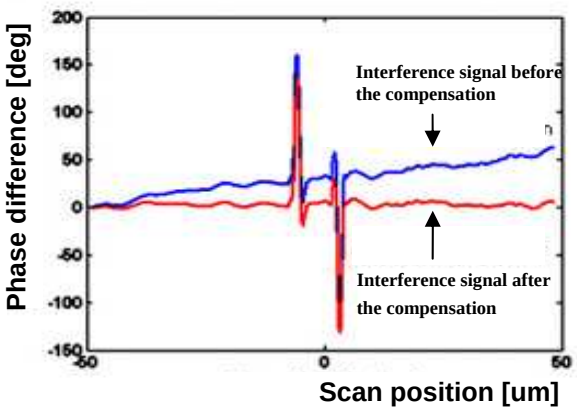


Figure.18 The compensation result of the interference signal measured in the middle of the field of view.

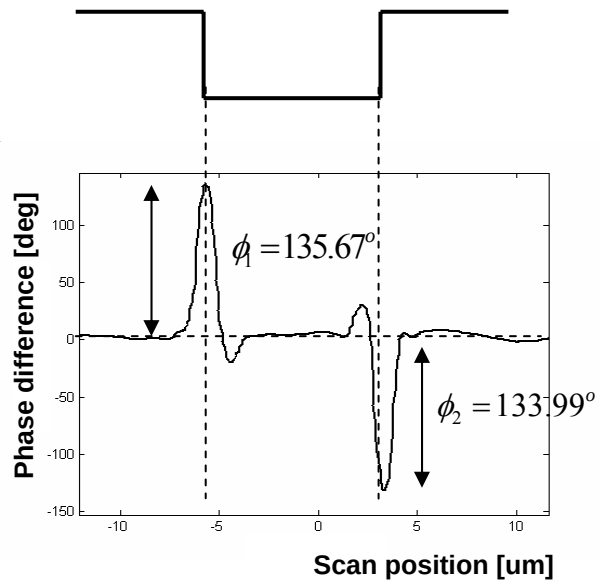


(a) Compensated interference signal

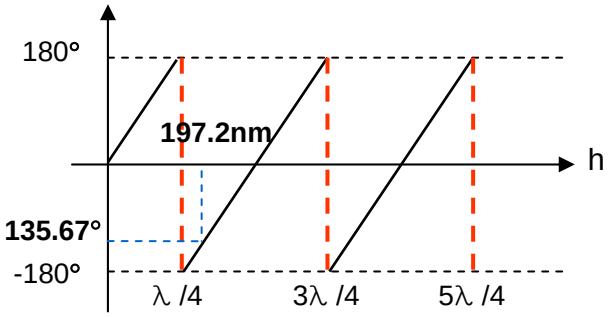


(b) Analysis by both interference and confocal signal

Figure.19 Measurement result in the middle of the field of view.